Neuron
Article

Cerebellar LTD and Pattern Recognition by Purkinje Cells

Volker Steuber,[1,3,7,*] Wolfgang Mittmann,[2,3,7] Freek E. Hoebeek,[4] R. Angus Silver,[3] Chris I. De Zeeuw,[4,5] Michael Häusser,[2,3] and Erik De Schutter[1,6]
[1] Laboratory of Theoretical Neurobiology, University of Antwerp, B 2610 Antwerp, Belgium
[2] Wolfson Institute for Biomedical Research
[3] Department of Physiology
University College London, London WC1E 6BT, United Kingdom
[4] Department of Neuroscience, Erasmus MC, 3000 DR Rotterdam, The Netherlands
[5] Netherlands Institute for Neuroscience (NIN), Royal Academy of Sciences (KNAW), 1105 BA Amsterdam, The Netherlands
[6] Computational Neuroscience Unit, Okinawa Institute of Science and Technology, Okinawa 904-0411, Japan
[7] These authors contributed equally to this work.
*Correspondence: v.steuber@herts.ac.uk
DOI 10.1016/j.neuron.2007.03.015

SUMMARY

Many theories of cerebellar function assume that long-term depression (LTD) of parallel fiber (PF) synapses enables Purkinje cells to learn to recognize PF activity patterns. We have studied the LTD-based recognition of PF patterns in a biophysically realistic Purkinje-cell model. With simple-spike firing as observed in vivo, the presentation of a pattern resulted in a burst of spikes followed by a pause. Surprisingly, the best criterion to distinguish learned patterns was the duration of this pause. Moreover, our simulations predicted that learned patterns elicited shorter pauses, thus increasing Purkinje-cell output. We tested this prediction in Purkinje-cell recordings both in vitro and in vivo. In vitro, we found a shortening of pauses when decreasing the number of active PFs or after inducing LTD. In vivo, we observed longer pauses in LTD-deficient mice. Our results suggest a novel form of neural coding in the cerebellar cortex.

INTRODUCTION

A fundamental assumption in neuroscience is that activity-dependent synaptic modifications represent a mechanism for storing information in the brain. One example of synaptic plasticity that has been implicated in learning and has received much attention is long-term depression (LTD) of synapses between parallel fibers (PFs) and Purkinje cells in the cerebellar cortex. PF LTD can be induced by repeated coincident PF and climbing fiber (CF) input to the Purkinje cell (Ito, 2001; Ito et al., 1982; Sakurai, 1987). Thus, a PF activity pattern that is paired repeatedly with CF input will lead to LTD of the PF synapses activated by the pattern. According to the classical view, this results in reduced simple-spike firing in the Purkinje cell when the PF activity pattern is presented again and thus leads to reduced inhibitory input to neurons in the deep cerebellar nuclei (DCN), increased output from the cerebellum, and execution of a movement (Boyden et al., 2006; Hansel et al., 2001; Ito, 1984; Ito, 2001; Jorntell and Hansel, 2006; Koekkoek et al., 2003; Mauk et al., 1998; Ohyama et al., 2003).

The hypothesis that PF LTD implements motor learning dates back to Marr and Albus's theoretical work (Albus, 1971; Marr, 1969), published long before Ito and collaborators found experimental evidence for the existence of LTD (Ito et al., 1982). This hypothesis has become known as the Marr-Albus theory (Ito, 1984) and forms the basis of many theoretical studies of cerebellar learning (for example, Gilbert, 1974; Medina et al., 2000; Schweighofer and Ferriol, 2000). All of these studies use very simplified Purkinje-cell models. In real Purkinje cells, the recognition of PF patterns is influenced by many factors, including the spatial distribution of inputs across the dendritic tree, the activation of voltage-gated ion channels, their modulation by cytoplasmic Ca^{2+} elevations, and the rate of simple-spike firing. Purkinje cells in vivo receive a background level of PF activity, which interact with intrinsic pacemaker currents to generate simple-spike firing at frequencies usually between 10 and 100 Hz (Armstrong and Rawson, 1979; Goossens et al., 2001). Thus, the weakening of the PF synapses by LTD must affect Purkinje-cell output in the context of continuous spiking. This raises the question of which features of the Purkinje-cell spike train could be used for recognizing learned PF patterns.

We studied the LTD-based recognition of PF activity patterns by analyzing simple-spike responses in a multicompartmental Purkinje-cell model with active dendrites and soma (De Schutter and Bower, 1994a; De Schutter and Bower, 1994b). We found that the best criterion for the recognition of patterns that had been learned by LTD

was the duration of the silent period after the pattern presentation, with learned patterns resulting in shorter pauses. These modeling predictions were confirmed with Purkinje-cell recordings in acute slices. As predicted, the length of the pause increased with PF stimulation strength and was shortened by an LTD induction protocol based on coactivation of PF and CF inputs. In agreement with this, a larger fraction of longer pauses in Purkinje-cell activity were observed in awake behaving mice deficient in LTD.

RESULTS

Pattern Recognition in the Purkinje-Cell Model

Figures 1 and 2 show the results of simulations where the Purkinje-cell model received a continuous background level of activation that caused it to fire simple spikes with an average frequency of 48 Hz, similar to mean firing rates observed in vivo. Learning of patterns was implemented as a reduction of the AMPA receptor conductances of activated PF synapses, as is the case after induction of LTD (see Experimental Procedures). All patterns comprised a set of PF inputs that were distributed randomly across the Purkinje-cell dendritic tree. In the first instance, we studied patterns in which 1000 randomly distributed PF synapses were activated synchronously. The model was presented with 75 of such PF patterns that had been learned by LTD, and its response was compared to the response to 75 novel patterns. As shown for the individual spike responses (Figure 1A) and the raster plot (Figure 1B), the Purkinje cell responded to both learned as well as novel patterns with a short burst of two or three simple spikes, and this was followed by a silent period of several tens of milliseconds.

On the basis of this characteristic response pattern, different features of the spike train were identified that could be used to discriminate between the responses to learned and novel PF input patterns. Figure 2 shows typical response distributions for three possible features: (1) the latency of the first spike fired in response to a pattern, (2) the number of simple spikes fired in a 25 ms time window after presentation of a pattern, and (3) the length of the simple-spike pause that followed the pattern presentation. For both the latency of the first spike (Figure 2A) and the number of spikes fired immediately after pattern presentation (Figure 2B), the distributions of responses to learned and novel PF patterns overlapped to a large degree. These overlapping response distributions resulted in low s/n ratios of 0.33 ± 0.17 for the spike latency and 0.21 ± 0.19 for the spike number (for n = 10 sets of 75 learned patterns). The best criterion for distinguishing learned and novel patterns was the length of the simple-spike pause. The two distributions of pause durations in response to learned and novel patterns were clearly separated (Figure 2C), resulting in an s/n ratio of 15.6 ± 2.6 (n = 10). Surprisingly, learned PF patterns resulted in shorter pauses (37.8 ± 6.0 ms) than novel patterns (56.6 ± 3.1 ms).

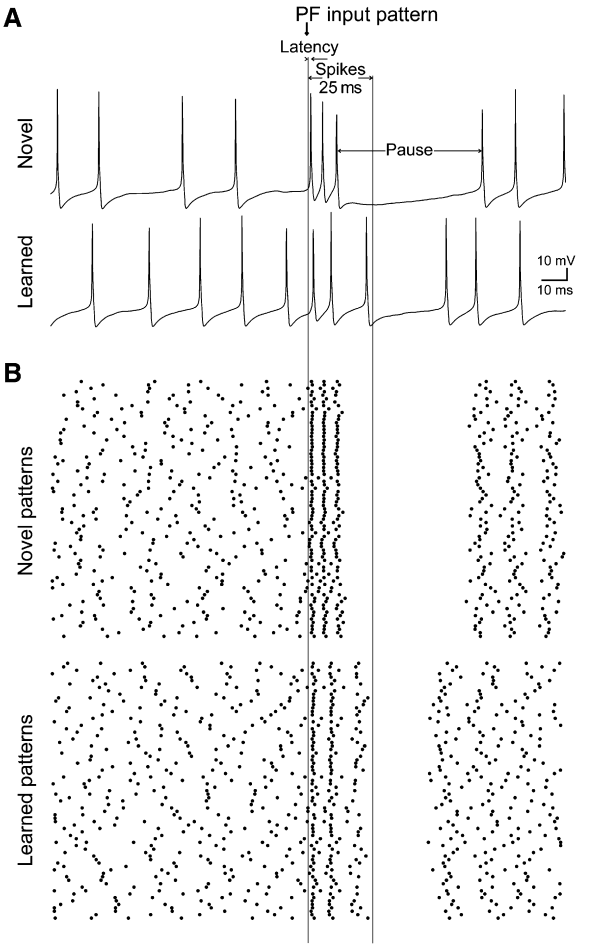

Figure 1. A Purkinje-Cell Model Responds to PF Input Patterns with a Burst of Simple Spikes Followed by a Pause

(A) Background PF activity resulted in a Purkinje-cell firing frequency of 48 Hz. Presentation of a novel and a learned PF input pattern evoked a burst of spikes followed by a pause. Note that the pause duration was reduced for the learned pattern.

(B) Raster plots showing the presentation of 75 learned and 75 novel PF activity patterns consisting of 1000 synchronously activated PF synapses. Same time scale as shown in (A).

Experimental Verification

We carried out experiments on Purkinje cells in cerebellar slices to test these modeling predictions. If, as the model predicts, the weakening of PF inputs by LTD results in shorter pauses after PF activation, stimuli that activate decreasing numbers of PFs should also lead to a decrease in the length of the pause. We made noninvasive extracellular recordings from spontaneously spiking Purkinje cells (Häusser and Clark, 1997; Walter et al., 2006; Womack and Khodakhah, 2003) and activated different numbers of PFs by using a range of stimulation strengths. To avoid pauses in spiking associated with feed-forward inhibition (Mittmann et al., 2005; Walter and Khodakhah, 2006), we blocked inhibition with SR95531 (10 μM).

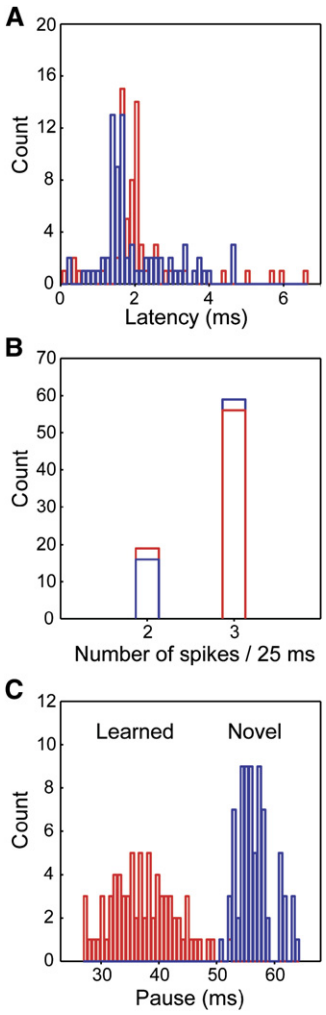

Figure 2. The Simple-Spike Pause Can be Used as Criterion to Distinguish Learned and Novel PF Activity Patterns

Panels show typical response distributions for the following three features of the spike train that could be used as criterion to recognize learned patterns: the latency of the first simple spike fired after presentation of a pattern (A), the number of spikes in the first 25 ms (B), and the length of the simple-spike pause after the pattern presentation (C). For the latency and spike number, the distributions of responses to learned (red) and novel (blue) patterns overlapped to a large degree, resulting in very low s/n ratios of 0.009 and 0.008, respectively. In contrast, for the pause, the two response distributions were clearly separated with an s/n ratio of 18.6. Simulation parameters are as shown in Figure 1.

At lower PF stimulation intensities (Figure 3A) the evoked burst of three or four spikes was followed by the normal spontaneous spiking of the Purkinje cell. When PF stimulation intensities were increased, a pause developed after the burst, and this pause was lengthened as stimulation strength was further increased. These pauses were of durations similar to those observed in the computer model (Figure 2C). Because extracellular recordings cannot resolve the size and properties of the underlying EPSPs, we subsequently made a whole-cell patch-clamp recording from the same Purkinje cell and recorded the EPSP (during hyperpolarizing current steps; Figure 3B). These whole-cell experiments also allowed us to rule out that the spike response was due to activation of the CF. In this (Figure 3C) and other cells (Figures 3D and 3E), we consistently found that the amplitude of the PF EPSP determined the length of the pause, quantified either as an absolute duration or normalized by the spontaneous ISI. In all cells, at least two different stimulation strengths produced pauses of different length ($p < 0.01$, $n = 10$) that were longer than the spontaneous ISI. All but one cell (9/10) responded to the next smaller EPSP with a significantly shorter pause (red connections in Figures 3D and 3E). The average increase in pause duration was 43% ± 10% for an underlying increase in EPSP amplitude of 52% ± 23% (n = 24 stimulation strengths in nine cells). Conversely, pauses triggered by different EPSP sizes did not differ significantly if the change in the underlying EPSP was small (−6% ± 2%, n = 10 stimulation strengths in five cells). It is possible that pauses, recorded extracellularly, were caused by synaptically induced transitions to silent downstates (Williams et al., 2002; Loewenstein et al., 2005). We tested this possibility by making whole-cell recordings, which showed a prolonged weak hyperpolarization associated with the pause, similar to the model and inconsistent with a downstate (Figure 3F, n = 4).

Under physiological conditions, the activation of a beam of PFs not only results in excitation of Purkinje cells but also activates inhibitory interneurons that make contacts with Purkinje cells situated on the same (Mittmann et al., 2005; Sultan and Bower, 1998) and on neighboring (Cohen and Yarom, 2000; Eccles et al., 1967) PF beams. It has recently been shown that PF stimulation in cerebellar slices activates feed-forward inhibitory input that arrives approximately 1 ms after the onset of the excitatory input to Purkinje cells (Brunel et al., 2004; Mittmann et al., 2005). In order to test whether feed-forward inhibition interfered with the positive relationship between EPSP amplitude and pause duration, we repeated the experiment in the presence of inhibition (i.e., without SR95531 in the bath). We found that when inhibition was intact, the length of the pauses in Purkinje-cell spiking increased with the magnitude of the EPSPs subsequently measured in whole-cell mode (Figures 3G and 3H). In all cells (7/7), one or more EPSPs evoked a significantly longer pause than the next smaller EPSP ($p < 0.01$). On average, the pause increased by 55% ± 19% for an underlying change in EPSP amplitude of 82% ± 13% (n = 23 stimulation strengths in seven cells). These experiments provide proof of principle that the pause in spiking after synchronous PF inputs provides a sensitive readout of PF EPSP size.

We next addressed the key prediction of the model by testing whether the same PF input would lead to a shorter pause after induction of LTD. Complex spikes were triggered by selectively activating the CF with an additional stimulation electrode. After a baseline period of 8–10 min, we paired PF and CF input with a temporal delay

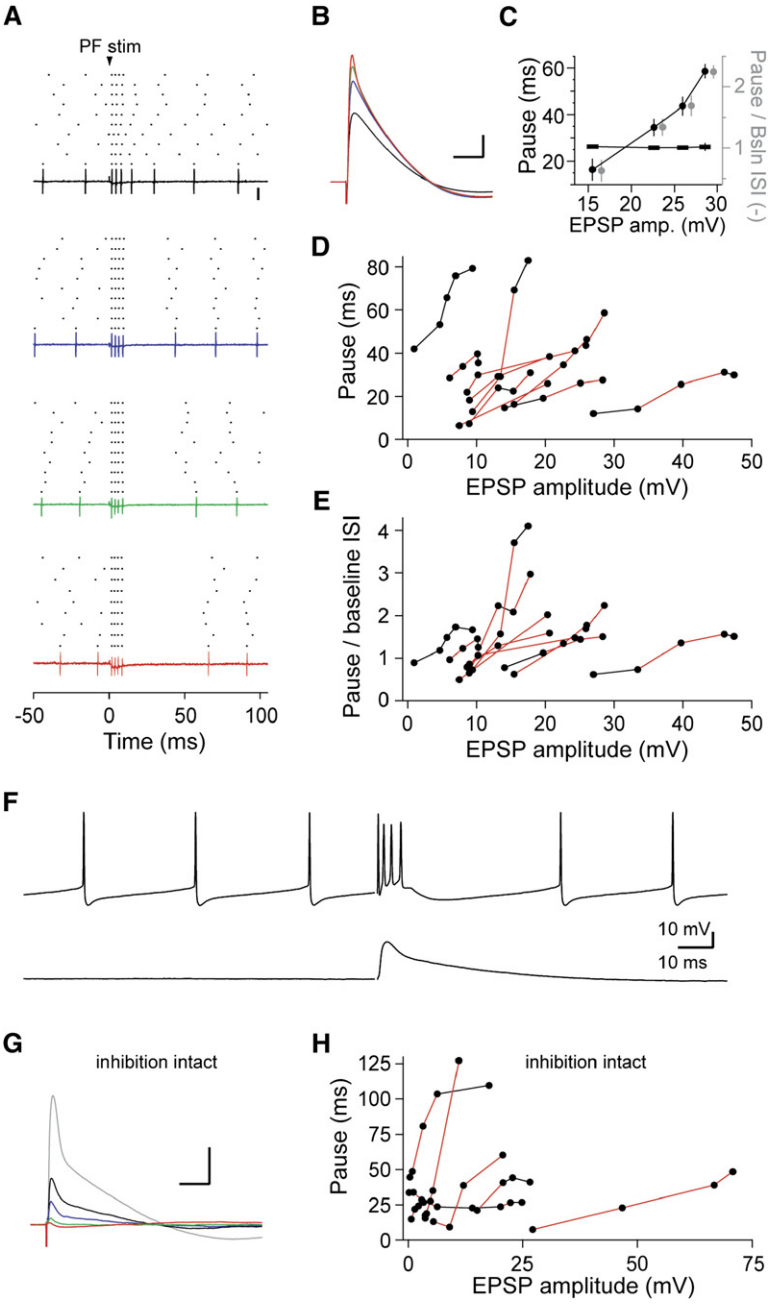

Figure 3. Synaptic Stimulation of Purkinje Cells in Acute Cerebellar Slices Evokes Bursts of Spikes Followed by Pauses

The data shown in (A)–(F) were recorded while inhibition was blocked by the addition of SR95531 to the bath. In (G) and (H), no SR95531 was added and inhibition was intact.

(A) Extracellular recording of spiking from a Purkinje cell in a cerebellar slice. A raster plot of ten consecutive sweeps is shown. The first sweep in each raster is also shown as a raw trace. The underlying EPSP amplitude for each raster was (top to bottom) 15.5, 22.6, 26.0, and 28.6 mV. The scale bar represents 200 pA and 100 pA for the last raw trace.

(B) After recording, spike data in cell-attached mode EPSPs at the respective stimulation strength were recorded in whole-cell mode. The scale bar represents 5 mV and 20 ms.

(C) Pause duration as function of EPSP amplitude (shown by black circles), baseline interspike interval (shown by rectangles), and pause divided by the interspike interval (shifted to the right for better visibility). Error bars indicate SE.

(D) Extracellularly recorded pause as function of EPSP amplitude in ten cells. Red connecting lines indicate statistical significance ($p < 0.01$).

(E) Same data as shown in (D), but normalized to the baseline interspike interval.

(F) A typical spiking trace recorded in whole-cell mode and the corresponding EPSP.

(G) EPSPs recorded at five different stimulation strengths with inhibition intact. The scale bar represents 5 mV and 20 ms.

(H) Pause duration as a function of EPSP amplitude in seven cells with inhibition intact.

of +1 ms for 300 times at 1 Hz (Sims and Hartell, 2005). This standard LTD induction protocol resulted in a reduction of the pause (Figures 4A and 4B), which developed in the first few minutes after LTD induction (Figure 4C). The average pause duration decreased from 82 ± 22 ms to 43 ± 9 ms after LTD induction, corresponding to a 65% ± 14% reduction (n = 6; Figure 4C). The change in the length of the pause was statistically significant in all but one case ($p < 0.001$; Figure 4D, left) where the pause length increased. Excluding this outlier, the s/n ratio for discrimination of pauses before and after the LTD induction protocol was 5.6 ± 1.3 (Figure 4D, right). Consistent with the model, other features of the spike train were poorer candidates for pattern recognition. The s/n ratios for the number of spikes in the burst (baseline: 3.8 ± 0.6 spikes; after induction: 3.4 ± 0.6 spikes) or the first spike latency (baseline: 1.8 ± 0.2 ms; after induction: 2.0 ± 0.2 ms) were less than two in all but one cell. The average s/n ratio was 1.0 ± 0.4 (outlier excluded) for the number of spikes in the burst and 0.34 ± 0.2 (outlier excluded) for the first spike latencies (Figure 4D). PF-evoked bursts (Figure 4E, top left) and CF responses (Figure 4E, top right) could be easily

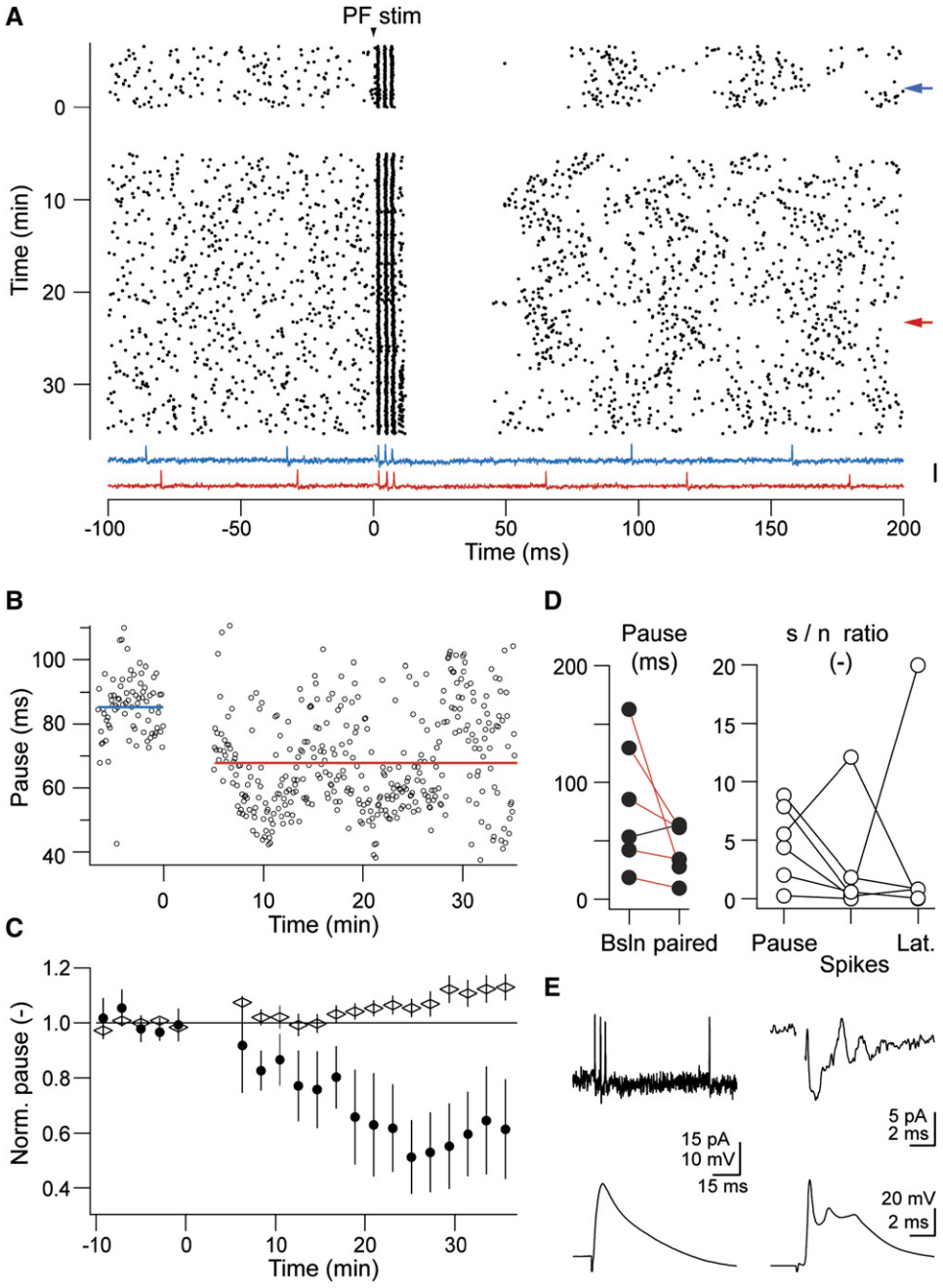

Figure 4. An LTD Protocol Leads to a Reduction in the Pause

(A) Spike raster showing the spiking pattern of a Purkinje cell in a cerebellar slice in response to PF stimulation before and after an LTD induction protocol (at t = 0 min) consisting of conjunctive PF and CF stimuli. Two sample traces at times indicated by the arrows show responses before (blue) and after (red) pairing. The scale bar represents 40 pA.

(B) The duration of the pause in spiking after PF stimulation plotted as a function of time relative to the LTD induction protocol.

(C) Averaged normalized pause length (shown by circles) and baseline interspike interval for six cells. Error bars indicate SE.

(D) Change of pause for single cells (red connection indicates statistical significance) and the corresponding s/n ratio of pause, number of spikes, and latency. Note that the cell with a low s/n ratio for the pause is the same cell that did not show a decrease in the pause in the left plot.

(E) Extracellularly recorded responses to PF and CF stimulation and the corresponding PF EPSP and complex spike recorded intracellularly in whole-cell mode (cell hyperpolarized to −69 mV) after collection of cell-attached data.

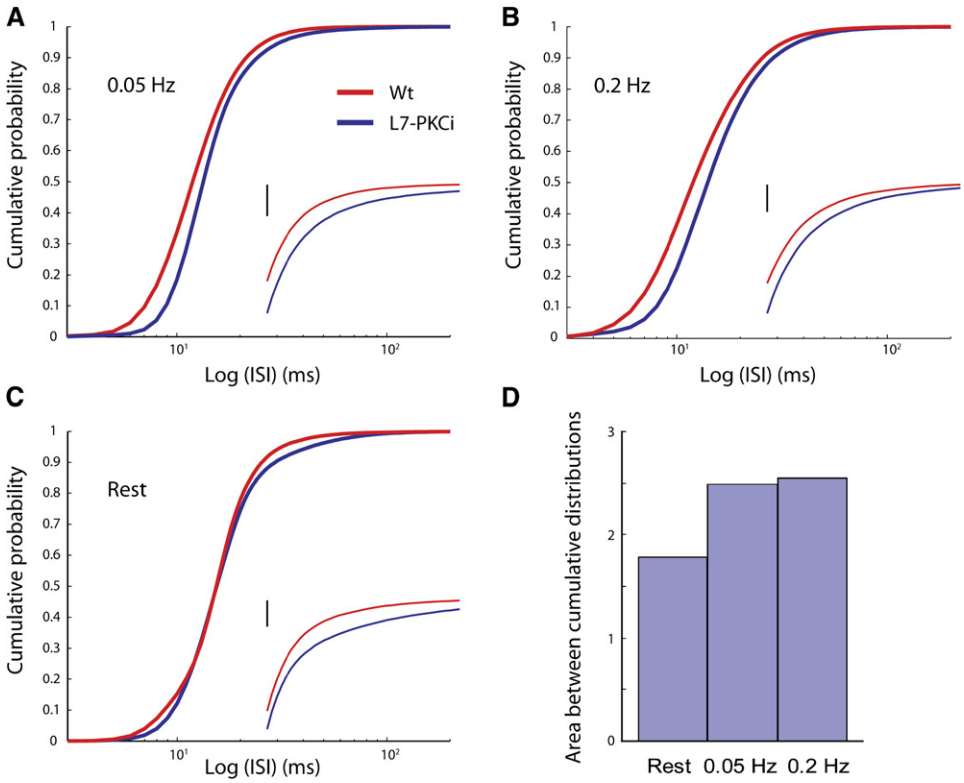

Figure 5. Increased Probabilities for Longer ISIs in LTD-Deficient L7-PKCi Mutants In Vivo

(A) and (B) show cumulative probability distributions for simple-spike firing of floccular Purkinje cells during sinusoidal optokinetic stimulation at 0.05 Hz (the wild-types are shown in red n = 7, L7-PKCi mutants are shown in blue n = 5) and 0.2 Hz (the wild-types, n = 13; L7-PKCi mutants, n = 9), respectively. (C) shows the same distributions of floccular Purkinje cells in the absence of optokinetic stimulation (the wild-types, n = 10; L7-PKCi mutants, n = 9). Insets indicate normalized probabilities for ISIs of 20–60ms (The scale bar represents 0.05.). (D) shows differences in surface areas between normalized cumulative probability distributions of the wild-types and L7-PKCi mutants during both the presence (0.05 Hz and 0.2 Hz) and absence (rest) of optokinetic stimulation. The LTD-deficient mutants show larger probabilities for longer ISIs under all circumstances, and these probabilities increase further during stimulation.

distinguished by the characteristic features of the CF response (including smaller spike amplitude, brief ISIs within the burst, low variability, and their all-or-none nature). After the induction protocol, we monitored pause duration for 30–40 min then repatched the same cell and recorded PF EPSPs (Figure 4E, bottom left) and CF responses (Figure 4E, bottom right) in whole-cell mode. This approach verified the nature of the extracellularly recorded spike responses (Figure 4E, top left). These experiments therefore confirm that an LTD induction protocol changes the pause in spiking as predicted by the model.

Floccular Purkinje-Cell Activity In Vivo

Our model and in vitro experiments suggest that the absence of LTD should lead to a higher incidence of longer ISIs in simple-spike firing. To find out whether such a correlation occurs in vivo, we analyzed the simple-spike activity of floccular Purkinje cells in awake behaving LTD-deficient L7-PKCi mutant mice responding to optokinetic stimuli (De Zeeuw et al., 1998; Goossens et al., 2004). Figure 5 shows that the simple-spike activities of LTD-deficient mutant mice indeed show increased probabilities for longer ISIs as compared to those of wild-type littermates. These differences were significant at optokinetic stimulation frequencies of both 0.05 Hz and 0.2 Hz (Figures 5A and 5B), and they held true both when tested for all ISI data represented in the probability distributions and when tested for an ISI range of 20–60 ms corresponding to the pause durations (in all cases, $p < 0.001$; Kolmogorov Smirnov test; Figures 5A and 5B). Moreover, although smaller, the same difference also occurred at rest ($p < 0.01$; Kolmogorov Smirnov test; Figures 5C and 5D). Thus, a Purkinje-cell-specific impairment of induction of LTD is associated with the expected altered simple-spike firing patterns at rest and is even more pronounced during natural sensory stimulation.

Mechanism of Pause Generation and Parameter Sensitivity

A possible mechanism for the generation of simple-spike pauses after PF activation was revealed by studying the Purkinje-cell model. In the compartmental model, the

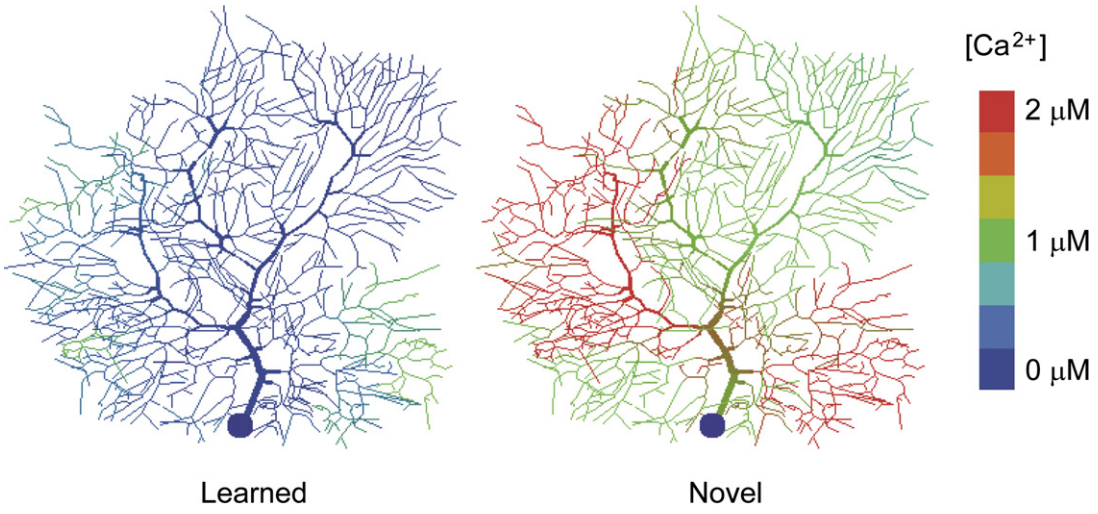

Figure 6. Learned PF Patterns Result in Less Ca^{2+} Influx in the Model than Novel Patterns

The Purkinje-cell model was presented with one of the learned patterns and a novel pattern, and a snapshot of the Ca^{2+} concentration in all compartments 10 ms after the pattern presentation is shown. Although the learned pattern also triggered an increase of the Ca^{2+} concentration compared to the resting level of 40 nM (left), the increase in response to the novel pattern was much greater (right). Same simulation parameters as in Figure 1.

basis of the pause generation is a negative-feedback process originating in the Purkinje-cell dendritic tree when sufficiently strong PF inputs trigger activation of voltage-gated Ca^{2+} channels (De Schutter and Bower, 1994c). This causes a short burst of somatic spikes (Figures 1, 3A, and 4A) and Ca^{2+} influx into the Purkinje-cell dendrites (Eilers et al., 1995). Dendritic Ca^{2+} responses to a learned and a novel pattern in the computer model are compared in Figure 6, and a movie showing the temporal evolution of the Ca^{2+} concentration in the dendritic tree is provided as Supplemental Data. PF patterns that had been learned by LTD resulted in less Ca^{2+} influx into the dendritic tree of the model. The Ca^{2+} influx led to activation of Ca^{2+}-dependent potassium channels and to a prolonged afterhyperpolarization (AHP, Figure 1A) (Cingolani et al., 2002; Etzion and Grossman, 1998; Fox and Gruol, 1993) that caused the pause by inhibiting spike generation. Because the amplitude and duration of the AHP was related to the amount of voltage-gated Ca^{2+} influx, LTD of AMPA receptor conductances resulted in shorter simple-spike pauses in the model.

Given that the generation of pauses in the model required sufficient Ca^{2+} influx into the dendritic tree, pattern recognition based on pause duration is only expected to work for PF patterns with a sufficiently large number of synchronously active synapses. In the simulations that were described previously (Figures 1, 2, and 6), we presented PF activity patterns in which 1000 of the 147,400 synapses were activated synchronously. This synchronous activity level of approximately 0.7% is similar to previous estimates of approximately 1% (Albus, 1971; Marr, 1969; Schweighofer and Ferriol, 2000) and is in agreement with a recent study showing optimal performance for activity levels of 0.2%–1% (Brunel et al., 2004). We studied the robustness of our predictions by varying the PF activity level and found that the predictions of the model held for patterns with at least 750 and not more than 8000 synchronously active synapses (Figure S1). Patterns in which the number of active PFs fell outside this range could not be discriminated.

Simulated Feed-Forward Inhibition

Our recordings from Purkinje cells in cerebellar slices with inhibition intact (Figures 3G and 3H) have shown that the presence of inhibition does not interfere with the positive relationship between effective PF input strength and pause duration. Given that the amplitude of feed-forward inhibitory input to Purkinje cells varies considerably from cell to cell (Mittmann et al., 2005), we explored the parameter dependence of the effect of inhibition on pattern recognition in the model. Figure 7 shows results of simulations in which the presentation of learned and novel PF patterns was followed by inhibitory input to the Purkinje cell with a delay of 1.4 ms (Mittmann et al., 2005) and varying strengths (see Experimental Procedures). The dependence of the inhibition/excitation ratio on the number of activated inhibitory synapses in these simulations was linear (Figure 7A). Moreover, inhibition/excitation ratios of up to two, which exceed the range of experimental observations for EPSPs > 4 mV (Mittmann et al., 2005), still permitted good pattern recognition on the basis of pause duration (Figure 7B). For larger inhibition/excitation ratios, the feed-forward inhibition resulted in deletion of spikes from the initial burst and increasingly variable pause durations (Figures 7C and 7D), similar to the effect of inhibition on response variability that has been demonstrated in previous studies (Häusser and Clark, 1997; Solinas et al., 2006). The increased variability of pause durations was

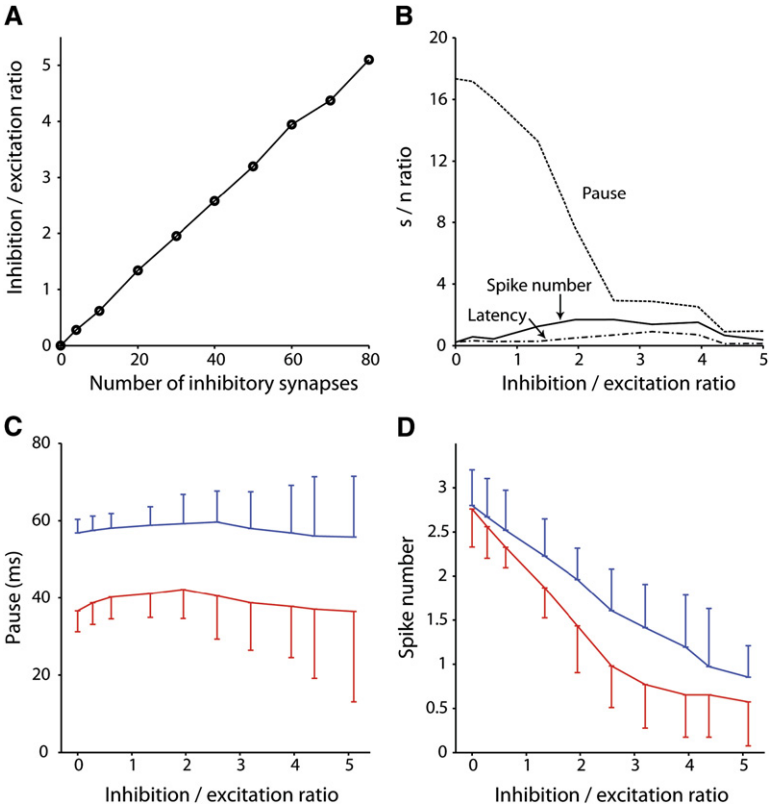

Figure 7. Feed-Forward Inhibition Does Not Affect the Model Predictions

The standard Purkinje-cell model learned 75 PF patterns with 1000 synchronously active synapses. The model was then presented with these learned patterns and the same number of novel patterns, each followed by input to a varying number of inhibitory synapses with a time delay of 1.4 ms (Mittmann et al., 2005). (A) shows the linear relationship between the number of inhibitory synapses activated and the inhibition/excitation ratio (see Experimental Procedures). (B) shows the dependence of pattern-recognition performance on the basis of pause duration, the number of spikes in the burst, and spike latency on inhibition/excitation ratio. Physiologically realistic inhibition/excitation ratios of up to two (Mittmann et al., 2005) resulted in good pattern separation on the basis of the duration of pauses. Pattern-recognition performance based on pause duration deteriorated not because of large changes in pause duration but because of increased variability (C). This variability occurred when strong inhibition reduced the number of spikes in the burst (D). Error bars in (C) and (D) indicate SD.

responsible for the small s/n ratios in the presence of strong inhibition (Figure 7B). Due to the deletion of spikes from the burst, increasing the level of inhibition initially increased the pause duration slightly both for learned and novel patterns (Figure 7C). A further increase in the inhibition/excitation ratio then resulted in shortening of pauses, presumably because of the decreased excitatory drive and reduced Ca^{2+} influx. However, these effects were small and the length of the pause (Figure 7C) was much less affected by the presence of feed-forward inhibition than the number of spikes in the burst (Figure 7D). We conclude that pattern recognition based on the duration of pauses is robust in the presence of feed-forward inhibition.

Pattern-Recognition Performance and Comparison with Simplified Models

An important issue in learning theory is the capacity of the storage system (Marr, 1969). We first evaluated this in the fully active Purkinje-cell model by computing s/n ratios for the three selected features of the spike response after having learned 10–300 patterns. Figure 8 shows that for learning of up to 150 patterns, the duration of simple-spike pauses resulted in s/n ratios of ten or greater, and it was clearly a better pattern-classification criterion than spike number and latency. For more than 150 learned patterns, the s/n ratio dropped to less than ten, and the pattern-recognition performance deteriorated. Figure 8 also compares the performance of the fully active model to that of a corresponding artificial neural network (ANN, see Experimental Procedures) and to pattern recognition on the basis of EPSP amplitudes in a nonspiking Purkinje-cell model where the soma had been made passive by removing all voltage-gated ion channels (Steuber and De Schutter, 2001). Both the ANN and the nonspiking Purkinje-cell model had much higher s/n ratios and therefore larger storage capacities than the more realistic active Purkinje-cell model with a full set of voltage-dependent ion channels.

Robust Pause-Based Pattern Recognition in the Presence of Spiking

Purkinje cells in vivo are characterized by their continuous irregular spiking, caused by a combination of intrinsic pacemaker currents and bombardment by PF background activity, and they show a wide spectrum of simple-spike rates between 10 and 100 Hz (Armstrong and Rawson, 1979; Goossens et al., 2001; Kahlon and Lisberger, 2000; Loewenstein et al., 2005; Murphy and Sabah, 1970; Shin et al., 2007). In order to determine the effect of the simple-spike firing rate on the recognition of patterns that had been learned by PF LTD, we presented 75 learned and 75 novel PF patterns to Purkinje-cell models that received background levels of PF activity between 0.20 and 0.56 Hz, thus resulting in simple-spike firing with average frequencies between 0 and 130 Hz

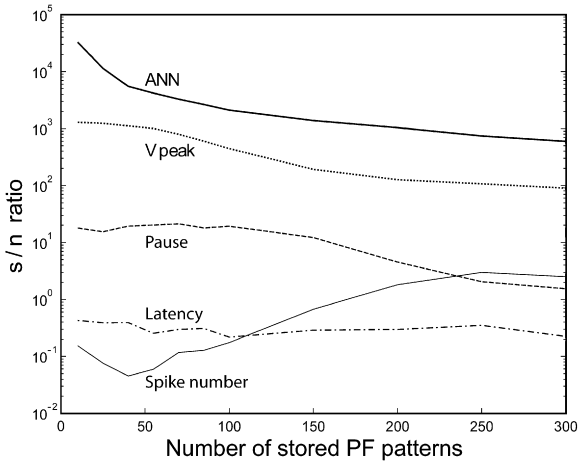

Figure 8. Dependence of Pattern-Recognition Performance on the Number of Learned Patterns

Between 10 and 300 patterns with 1000 synchronously active PF inputs were learned by the standard Purkinje-cell model. The model was presented with the learned patterns and with the same number of novel patterns, and the pattern-recognition performance was evaluated by the calculation of s/n ratios for three response criteria. The performance of the spiking model was compared with the corresponding artificial neural network (ANN, see Experimental Procedures) and with pattern recognition on the basis of the amplitude of the voltage response in a nonspiking Purkinje-cell model with a passive soma (Vpeak, see Steuber and De Schutter, 2001). Note the logarithmic scale of the y axis. Simulation parameters are as shown in Figure 1.

(Figure 9A). We found an interesting dichotomy between the silent and firing modes of the Purkinje-cell model. Only models in which the PF background rate was too low to result in simple-spike firing behaved in agreement with classic cerebellar learning theories. In these unphysiologically silent models, both the latency of the first spike and the number of spikes in the first 25 ms after presentation of a pattern could be used to distinguish between learned and novel patterns, with longer latencies and less spikes in response to learned patterns. In contrast, in firing Purkinje-cell models, only the length of the simple-spike pause could be a criterion for pattern classification. Under these conditions, which mimic the in vivo situation, an increase in simple-spike-firing rates resulted in greater s/n ratios. Thus, the duration of pauses provides a robust pattern-recognition criterion in the presence of ongoing neuronal activity, with an increasing amount of PF background input leading to better performance. This is in direct contrast to pattern recognition in an ANN, where increasing the level of noise by increasing the background input caused a degradation of performance (Figure 9B).

Sensitivity to Noise

We then studied the effect of different types of noise that could interfere with pattern recognition in Purkinje cells in vivo. An important source of noise is fluctuations in the size of postsynaptic responses (Kreitzer and Regehr, 2000; Nusser et al., 2001; Silver et al., 1998; Wall and Usowicz, 1998). In Purkinje-cell recordings in cerebellar slices, both spontaneous glutamatergic currents and currents evoked by stimulation of individual granule cells are highly variable (Barbour, 1993; Isope and Barbour, 2002). This trial-to-trial variability of postsynaptic responses is expected to have an influence on the recognition of PF patterns. Moreover, another source of noise that could influence pattern recognition in Purkinje cells is the variable extent of AMPA receptor LTD induced for each of the active PF inputs in a pattern (see e.g., Figures 5 and 6 in Wang et al. [2000] and Figures 3–5 in Xia et al. [2000]). The effects of both quantal variance of the AMPA receptor conductance and variability of AMPA receptor LTD are shown in Figure 9C. Quantal variance with a coefficient of variation (CV) of 0.5, variable LTD with a CV of 0.5, or a combination of both did not cause a significant drop in pattern recognition performance.

In addition to noise in the amplitude of the individual postsynaptic responses, there could also be noise in the timing of the afferent input. Up to now we have assumed that a Purkinje cell has to recognize PF activity patterns composed of the synchronous activation of a number of PF synapses. Figure 9D demonstrates the effect of temporal jitter in the PF input patterns. The individual PF inputs in a pattern could be desynchronized over a time window of up to 8 ms before the discrimination between learned and novel PF patterns became impossible.

DISCUSSION

Our simulations and experimental results suggest a novel readout of information storage in cerebellar Purkinje neurons, in which synaptic weights are encoded in a pause in spiking after synchronous synaptic activation. Surprisingly, this mechanism more sensitively reflects the strength of PF synapses than do the spikes directly triggered by the synaptic input. This is in contrast to prevailing theories of cerebellar learning and provides a new perspective on the cellular basis of motor learning.

LTD Decreases the Duration of Simple-Spike Pauses

LTD of the synapses between PFs and Purkinje cells is assumed to be one of the substrates of learning in the cerebellar cortex. According to classic theories of cerebellar learning, a Purkinje cell can store and learn to distinguish PF activity patterns that have been presented repeatedly together with CF input to the cell (Albus, 1971; Ito, 1984; Marr, 1969). The resulting LTD of the PF synapses is assumed to lead to a decreased rate of Purkinje-cell simple-spike firing, a reduction in the inhibition of their target neurons in the deep cerebellar nuclei (DCN), and thus an increased output from the cerebellum (Boyden et al., 2006; Hansel et al., 2001; Ito, 1984; Ito, 1989; Ito, 2001; Jorntell and Hansel, 2006; Koekkoek et al., 2003; Mauk et al., 1998; Ohyama et al., 2003; Thompson and Krupa, 1994). The main prediction of our combined computer

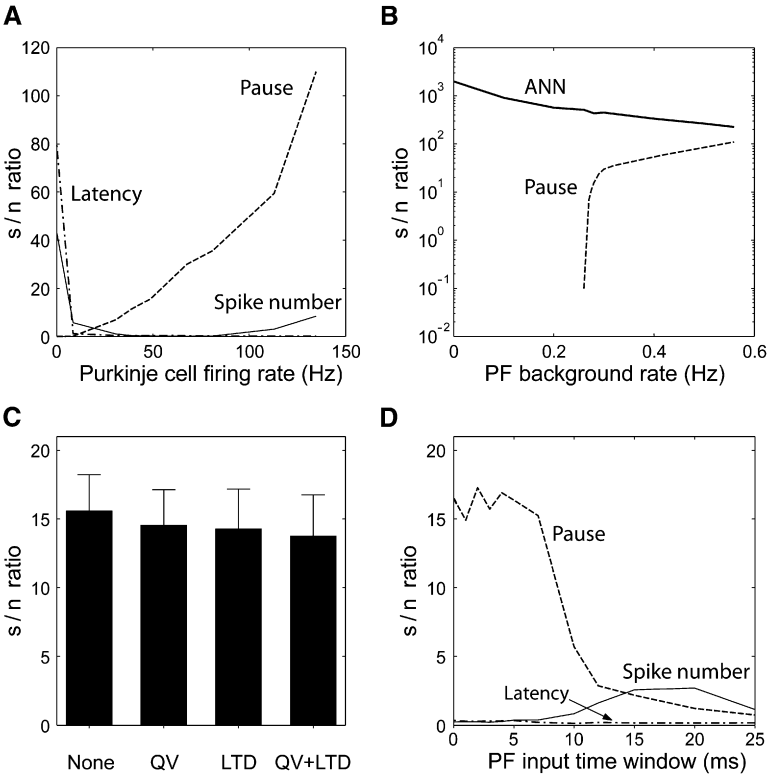

Figure 9. Influence of Firing Rate and Different Forms of Noise on the Pattern-Recognition Performance

(A) Purkinje cell models that received 0.2-0.56 Hz PF background input and fired simple spikes with frequencies between 0 and 130 Hz learned 75 patterns with 1000 synchronously active PFs. The models were presented with the 75 learned and 75 novel patterns, and the pattern-recognition performance was evaluated for the three response criteria. Only silent Purkinje-cell models could use the latency and spike number for pattern recognition. Purkinje-cell models that fired simple spikes could only use the pause, with increasing firing rates resulting in an improved pattern-recognition performance.

(B) The effect of PF background activity on pattern recognition based on pauses in the Purkinje-cell model is compared to the effect of a corresponding form of noise in the ANN (see Experimental Procedures).

(C) The Purkinje-cell model was presented with the 75 learned patterns and 75 novel patterns under conditions in which the individual AMPA receptor mediated postsynaptic currents were variable (quantal variance, QV) or the extent of LTD induced was variable, both with a coefficient of variation of 0.5. Simulation parameters are as shown in Figure 1. Error bars indicate SD.

(D) The model was presented with 75 learned and 75 novel patterns with 1000 active PF inputs that contained temporal jitter, introduced by randomly distributing the different active inputs in a pattern over time windows between 0 and 25 ms. Simulation parameters are as shown in Figure 1.

modeling and experimental study is that the readout of learned patterns in Purkinje cells may operate in a fundamentally different way.

We first studied the recognition of PF activity patterns that had been learned by LTD of AMPA receptor conductances in a biophysically realistic Purkinje-cell model. On the basis of simulations where combined excitatory and inhibitory background input resulted in continuous simple-spike firing as observed in vivo (De Schutter and Bower, 1994b; Jaeger et al., 1997), the model predicted that synchronized PF inputs trigger a short burst of spikes followed by a pause. The dominant effect of LTD based on a decrease of the AMPA receptor conductances was a shortening of the pause. This prediction was confirmed with noninvasive extracellular recordings from Purkinje cells in cerebellar slices. We first verified that strong synchronous stimulation of PF input triggers subsequent pauses in spontaneous firing, in agreement with a recent report (Lev-Ram et al., 2003), as well as with in vivo extracellular recordings from Purkinje neurons (Bower and Woolston, 1983). Next, we showed directly that LTD induction reduced postburst pause duration and that the first spike latency and the number of spikes in the burst are poorer candidates for pattern recognition compared to the pause. Although consistent with the model, this is a somewhat surprising result given that Lev-Ram and colleagues used the number of spikes in the burst to monitor amplitudes of PF EPSPs (Lev-Ram et al., 2003). The smaller reduction in the number of spikes in the burst after LTD induction we have observed (15% compared to 35% in their study) may be related to the different induction protocol or the more physiological temperatures used in our experiments. Our in vitro experiments thus support the modeling results, showing that the duration of the pause is the best candidate for pattern recognition.

Further support for the predicted shortening of pauses by LTD was found in simple-spike activity of Purkinje cells from awake behaving mice during optokinetic stimulation. LTD-deficient mice showed higher probabilities for longer pauses than wild-type mice, and such a finding is in agreement with our simulation results and in vitro data. Moreover, the difference between the mutant mice and their wild-type littermates was more pronounced during optokinetic stimulation than during rest, and this could fit with a possible behavioral relevance of the pauses. Future in vivo studies, in which pauses are measured during a learning task such as visuovestibular training (see e.g., Schonewille et al. [2006]), will be needed to provide

more direct evidence for the relevance of pauses in vivo and their shortening by LTD induction.

Mechanism of Pause Generation and Parameter Sensitivity

The generation of simple-spike pauses in the model was based on Ca^{2+} influx through high-voltage-activated P-type Ca^{2+} channels, which activated Ca^{2+}-dependent K^+ (KCa) channels. This resulted in a prolonged AHP, which inhibited spike generation and caused a pause in firing. In the model, the amount of Ca^{2+} influx and therefore the duration of pauses increased with the effective PF input strength and was reduced by LTD (Figure 6). In the experiments, the activation of KCa channels could not only be observed as an AHP in super-threshold responses (Figure 3F) but was also reflected by the faster initial decay of larger EPSPs (Figures 3B and 3G).

Pauses only occurred in the model when sufficiently strong PF inputs triggered sufficient Ca^{2+} influx into the dendritic tree. Similarly, weak PF stimulation did not result in pauses in our experiments (Figure 3A). This is in agreement with a recent study showing that pauses were only generated for larger PF stimulation intensities, with increasing stimulation strengths resulting in longer pause durations (Walter and Khodakhah, 2006). Interestingly, this study also reported AHPs in response to strong PF inputs (Figure S3 in their study). It is conceivable that Purkinje cells decode weak and strong PF inputs in different ways. In our model, pause-based pattern recognition was possible for PF patterns in which at least 750 out of all 147,400 synapses were activated (Figure S1). This corresponds to an activation probability of approximately 0.5%, which is a similarly low activation probability as that for the sparse patterns that have been used in other models of cerebellar learning (Albus, 1971; Brunel et al., 2004; Marr, 1969; Schweighofer and Ferriol, 2000). Although it is difficult to estimate exactly how many PFs were activated in the experiments, a unitary EPSP of 0.07 mV (Isope and Barbour, 2002) would suggest approximately 290 PFs are required for a 20 mV EPSP. However, this linear estimate is likely to be a lower limit given that shunting effects and reductions in driving force are associated with large inputs.

Pattern recognition based on pauses required roughly similar numbers of active PFs in models and experiments. However, the spatial pattern of the inputs in the model and experiments may be different. Inputs were randomly distributed over the dendritic tree in the model, but PF stimulation is likely to result in the activation of PF synapses confined to a smaller area of the Purkinje-cell dendrite. Such clustered input has been suggested to result in higher local glutamate concentrations (Marcaggi and Attwell, 2005) and stronger local depolarization and Ca^{2+} influx (Wang et al., 2000). Clustered input could therefore result in a lower threshold for pause generation and pause signaling. Such a reduction in threshold is also likely to be accompanied by a reduction in the dynamic range because saturation effects will be more pronounced for clustered inputs. Consistent with this speculation, we found that in the model the s/n ratio rapidly decreased when inputs were clustered (data not shown). This suggests that in vivo Purkinje cells, which are likely to receive a distributed input, can outperform the average s/n ratio of six we observed with focal stimulation in vitro.

We also studied the effect of feed-forward inhibition on pattern recognition and found that the pattern-recognition performance was very robust against the presence of feed-forward inhibition. Physiologically relevant inhibition/excitation ratios of up to two (Mittmann et al., 2005; Walter and Khodakhah, 2006) still resulted in good pattern separation (Figure 7). These simulation results are consistent with our experimental data showing that the dependence of pause duration on effective PF input strength is unaffected by the presence of feed-forward inhibition (Figures 3G and 3H). We did not include plasticity of the synapses between PFs and inhibitory interneurons (Jorntell and Ekerot, 2002; Jorntell and Ekerot, 2003; Rancillac and Crepel, 2004; Smith and Otis, 2005) in our simulations because there is currently insufficient data available to build realistic models of these synaptic mechanisms, and their potential involvement are beyond the scope of this study.

The Role of Purkinje-Cell Spiking and Noise

Existing theories of cerebellar learning tend to underestimate the amount of noise and often fail to take the continuous simple-spike firing in Purkinje cells into account. A recent study of pattern storage in Purkinje cells (Brunel et al., 2004) has suggested that each Purkinje cell could learn to recognize approximately 40000 different PF input patterns. However, this is on the basis of the assumptions that the Purkinje-cell output is binary and that the combined noise sources result in a SD of $\sigma \leq 0.4$ mV. The presence of PF background input and continuous firing drastically reduces the number of associations that can be learned in the more realistic Purkinje-cell model used in this study and makes it necessary to analyze its response over a longer time period; this invalidates the assumption that a Purkinje cell can be simplified to a binary threshold unit. Moreover, in a situation where the relevant Purkinje-cell output is the duration of simple-spike pauses, different types of noise can have very different and sometimes counterintuitive effects. Our simulations predict that pattern recognition based on the duration of pauses is very robust in the presence of continuous spiking. Furthermore, an increasing amount of PF background activity led to an improved pattern-recognition performance. Although surprising at first glance, the beneficial effect of this kind of noisy synaptic input can be understood by considering that a higher PF background rate decreases the variance in the length of simple-spike pauses, and this results in an increased s/n ratio. Our study demonstrates that a biophysically realistic Purkinje-cell model that has been tuned to reproduce realistic in vivo behavior can lead to completely different predictions than simplified ANNs and models that do not fire spontaneously.

In the presence of tonic firing, the influence of other kinds of noise was rather weak. It has been argued that the commonly observed trial-to-trial fluctuations in the amplitude of postsynaptic responses present a problem for the storage of information in synaptic weights (Poirazi and Mel, 2001). Contrary to this suggestion, we found that quantal variance of the AMPA receptor conductance resulted in a surprisingly small decrease in pattern-recognition performance. A similarly small drop in performance was observed in the presence of variable AMPA receptor LTD. The predictions of the model are very robust against these forms of synaptic noise.

Decoding Simple-Spike Pauses

Our study suggests that the duration of simple-spike pauses provides a better coding mechanism than spike number or latency. Similarly, another spike-response feature, the rate of simple spikes in the burst after pattern presentation, also resulted in poor pattern separation with an s/n ratio of 1.4 ± 0.6. Apart from the low s/n ratio, the intra burst frequency is likely to be too high to reliably propagate along the Purkinje-cell axon (Monsivais et al., 2005). This supports the view that the spike frequency within the burst as well as the number of spikes are less useful than pauses for distinguishing between learned and novel patterns over the range of PF excitation examined in this study. A consequence of a pause-based coding mechanism is that the readout is considerably slower than possible for spike number or latency-based mechanisms.

Our prediction that the duration of simple-spike pauses could provide an important output from the cerebellar cortex raises the question of how simple-spike pauses can be decoded by neurons in the DCN. DCN neurons follow hyperpolarizing current pulses with a rebound depolarization (RD), which often triggers a burst of action potentials (Aizenman and Linden, 1999; Aizenman et al., 1998; Czubayko et al., 2000; Jahnsen, 1986; Llinas and Muhlethaler, 1988; Mouginot and Gahwiler, 1995; Muri and Knopfel, 1994). Even stronger RDs can be elicited by trains of inhibitory postsynaptic potentials (IPSPs) that originate from Purkinje-cell inputs (Aizenman and Linden, 1999; Aizenman et al., 1998; Gardette et al., 1985; Llinas and Muhlethaler, 1988). Aizenman and Linden (1999) have suggested that DCN neurons could use the RD to distinguish between PF and CF input to their presynaptic Purkinje cells. They propose that the continuous simple-spike firing in the Purkinje cells results in tonic inhibition of the DCN neurons. In contrast, CF input leads to a complex spike followed by a silent period in the Purkinje cell and could elicit a RD. Similarly, a RD in a DCN cell would be expected when the presynaptic Purkinje cells are presented with a pattern of synchronous PF inputs. Given that learned PF patterns lead to shorter simple-spike pauses than novel patterns, they should also trigger RDs with shorter bursts of action potentials. Thus, we expect PF activity patterns that have been learned by LTD at the PF–Purkinje-cell synapses to result in decreased output from the DCN.

Further Predictions

We have shown that PF LTD can result in a shortening of simple-spike pauses evoked by PF input and that this shortening of the pauses is the most significant consequence of LTD induction. If our predictions are correct, and cerebellar learning is based on a modulation of the duration of silent periods, any pharmacological intervention that interferes with the generation or modulation of the pauses should also inhibit learning. Interestingly, a recent study (Koekkoek et al., 2005) has shown that eye-blink conditioning can be impaired by an increase of the magnitude of LTD. A possible explanation based on our results is that an excessive shortening of pauses due to strong LTD makes them indistinguishable from normal ISIs.

In order for the modulated pauses to have any effect on cerebellar output, pauses in Purkinje cells converging onto common DCN neurons would have to be synchronized. Consistent with this, in vivo recordings of nearby Purkinje cells in anaesthetized rats have revealed that greater than 10% of pauses are synchronized (Shin and De Schutter, 2006). However, it has been shown that anesthesia can affect the Purkinje-cell firing pattern (Schonewille et al., 2006). Further studies, both in anaesthetized and awake behaving animals, are required for investigating the synchronization of Purkinje-cell pauses and the output of the DCN after LTD and how they contribute to cerebellar learning.

EXPERIMENTAL PROCEDURES

The Purkinje-Cell Model

Simulations were performed with the GENESIS simulator (Bower and Beeman, 1998). Unless stated otherwise, we used the multicompartmental Purkinje-cell model with active dendrites and soma that has been previously described in detail (De Schutter and Bower, 1994a; De Schutter and Bower, 1994b; see Supplemental Experimental Procedures). Purkinje cells receive PF synapses on approximately 150,000 dendritic spines (Harvey and Napper, 1991). Given that it is computationally very expensive to simulate such a large number of spines, two different versions of the Purkinje-cell model were used. In an initial set of simulations, 147,400 spines were modeled. All spines were activated independently by a random sequence of PF inputs with an average rate of 0.28 Hz. This background excitation was balanced by tonic background inhibition, and the standard model fired simple spikes at an average frequency of 48 Hz. We simplified the model by reducing the number of spines while at the same time increasing the rate of PF background excitation. In the simplified model, only 1474 spines were represented explicitly. Each of these spines was activated at an average frequency of 28 Hz and, like the full model, the simplified model fired simple spikes at an average rate of 48 Hz. The initial pattern-recognition simulations (Figures 1 and 2) were run for both models. Given that the simplified model and the full model produced identical results, only the simplified model was used for the parameter search simulations (Figures 6–9). The validity of this simplification has also been shown previously (De Schutter and Bower, 1994b).

In a set of control simulations, the effect of different levels of feedforward inhibition was studied by activating a variable number of inhibitory synapses on the soma and main dendrite (De Schutter and Bower, 1994b). In these simulations, we verified inhibition/excitation

ratios by voltage-clamping the model to −40 mV, i.e., half way between the excitatory and inhibitory reversal potentials, and measuring the ratios of the mean IPSC peak to the mean EPSC peak. The inhibitory input followed the synchronous activation of excitatory PF synapses with a delay of 1.4 ms (Mittmann et al., 2005) and had a rise time constant of 1 ms and a decay time constant of 8 ms (W.M. and M.H., unpublished data).

Pattern Recognition

Learning of PF activity patterns in the Purkinje-cell model was simulated in two steps. In the first step, binary input patterns were generated and learned by a corresponding artificial neural network (ANN). The resulting vector $\boldsymbol{w}$ of synaptic weights was then transferred to the Purkinje-cell model. This two-step procedure mimics the direct learning of PF patterns by depressing the AMPA receptor conductances in the Purkinje-cell model and makes it easier to compare the performance of the two models. The ANN and the analysis of the results were implemented in C++.

Storage and Recognition of Input Patterns in the ANN

The ANN has been described previously in a study of pattern recognition in nonspiking Purkinje-cell models with a passive soma (Steuber and De Schutter, 2001). It is a modified version of an associative network (Willshaw et al., 1969) with real valued synapses and an LTD learning rule and resembles the models that have been used in classical studies of cerebellar learning (Albus, 1971; Gilbert, 1974; Marr, 1969). We used a network with 147,400 synapses, corresponding to the number of PF inputs in the Purkinje-cell model, and stored (learned) between 10 and 300 binary PF input patterns. Each of the binary input patterns was a vector with N elements in randomly chosen locations that represented active PFs and were set to 1, and 147,400–N elements that represented inactive PFs and were set to 0. Initially, all PF synaptic weights were set to 1. When a PF input pattern was presented together with a CF signal, the pattern was learned by the decrease of the synaptic weights w_i that were associated with active PFs to 50% of their previous values. Learned PF patterns were encoded in the resulting vector $\boldsymbol{w}$ and could be recalled in the absence of CF input. The response of the ANN was given by the sum of the weights of all synapses that receive PF input. The ANN was presented with the patterns that had been learned and with the same number of novel patterns, which also contained N elements in randomly chosen locations that were set to 1 and 147,400–N elements that were set to 0. The average level of response to learned patterns was lower than the response to novel patterns, and the ability of the net to discriminate between learned and novel patterns could be described by the calculation of a signal-to-noise ratio (Dayan and Willshaw, 1991; Graham, 2001):

$$s/n = \frac{2(\mu_l - \mu_n)^2}{\sigma_l^2 + \sigma_n^2}$$

where μ_l and μ_n are the mean values, and σ_l^2 and σ_n^2 are the variances of the response to learned and novel patterns, respectively. In a series of control simulations, the effect of noise in the ANN was studied (Supplemental Experimental Procedures).

Pattern Recognition in the Purkinje-Cell Model

Before learning, all PF synapses of the Purkinje-cell model activated the same maximum AMPA receptor conductance $\bar{g}_0 = 0.7nS$ (De Schutter and Bower, 1994b). Copying the synaptic weights w_i from the ANN to the Purkinje-cell model to mimic learning resulted in synapse-specific AMPA receptor conductances that were given by $\bar{g}_i = w_i \bar{g}_0$. In analogy to the ANN, the learned PF patterns in the Purkinje-cell model were encoded by the synaptic conductances and could be recalled without coincident CF input. For each of the binary input patterns in the ANN, the Purkinje-cell model was presented with a corresponding pattern of AMPA receptor activation by PF input, and the pattern-recognition performance was evaluated by the calculation of s/n ratios for the spike response's different features, including the latency of the first spike fired in response to a PF pattern, the number of spikes fired in a 25 ms time window after presentation of a pattern, and the length of the simple-spike pause that followed the pattern presentation. Pauses were defined as the first silent period after pattern presentation that exceeded the mean baseline ISI before pattern presentation. In cases where the presence of strong inhibition resulted in the absence of a spike response immediately after pattern presentation, the pause duration was measured starting from the first spike before pattern presentation.

In a previous study of LTD-based pattern recognition in a nonspiking Purkinje-cell model with a passive soma, we observed the best performance for PF patterns where N = 1000 inputs (i.e., approximately 0.7% of the 147,400 inputs) were active synchronously (Steuber and De Schutter, 2001). This number of active inputs is very similar to previous estimates (Marr, 1969; Albus, 1971; Schweighofer and Ferriol, 2000; Brunel et al., 2004). Most of the simulations presented here also used PF patterns consisting of the synchronous activation of 1000 synapses. In a set of control simulations, the number of active PF synapses per pattern was varied, and in another set of simulations, the active inputs were desynchronized by random distribution of them over time windows of up to 25 ms. In the full Purkinje-cell model, each of the 147,400 spine heads contained one PF synapse. In the simplified model with 1474 spines, each of the spine heads received input from 100 PFs with different synaptic weights. Pattern-recognition simulations with both models produced the same results.

Purkinje-Cell Recordings In Vitro

We recorded from visually identified neurons in 300-μm-thick sagittal slices of the cerebellar vermis. Slices were prepared from 18- to 24-day-old Sprague–Dawley rats anaesthetized via isoflurane inhalation as previously described (Häusser and Clark, 1997; Stuart et al., 1993), in accordance with institutional and national regulations. Slices were continuously perfused with artificial cerebrospinal fluid (ACSF) containing 125 mM NaCl, 26 mM $NaHCO_3$, 25 mM glucose, 2.5 mM KCl, 1.25 mM NaH_2PO_4, 2 mM $CaCl_2$, and 1 mM $MgCl_2$ bubbled with 95% O_2/5% CO_2. Neurons were identified and recordings were made under direct visual control with infrared differential-interference-contrast optics on an upright microscope (Axioskop, Zeiss). All experiments were performed at 34.2°C ± 0.2°C.

Electrophysiological recordings from Purkinje cells were made with a Multiclamp 700A amplifier (Axon Instruments). Pipettes were pulled to a resistance of 2–6 MΩ, used for loose cell-attached and whole-cell current-clamp recordings, and filled with ACSF or a solution containing 130 mM methanesulfonic acid, 10 mM HEPES, 7 mM KCl, 2 mM Na_2ATP, 2 mM MgATP, 0.4 mM Na_2GTP, 0.05 mM EGTA, and biocytin (0.4%), respectively. In whole-cell recordings, pauses after bursts evoked by PF stimulation decreased gradually with time. Pause durations did not change systematically in cell-attached recordings with seal resistances between 10 and 100 MΩ. Tight seals were avoided because they often resulted in spontaneous transitions to the whole-cell configuration. Liquid junction potentials were not corrected for. Parallel fibers were stimulated with pipettes containing ACSF placed >50 μm below the dendritic tree of the recorded cell so that activation of the CF could be avoided. CFs were activated with a second ACSF-filled electrode placed in the granule cell layer. $GABA_A$ receptors were blocked by bath application of the specific antagonist SR95531 ("SR") (Hamann et al., 1988), except when otherwise noted. Data were low-pass filtered at 4–10 kHz and sampled at 20 kHz with a 1321A Digidata A/D converter (Axon Instruments). Data were analyzed offline with Igor Pro (Wavemetrics). Data are presented as mean ± SE, and statistical significance was tested with the Student's unpaired t test. Data in Figure 4C were averaged over 2 min bins, and statistical significance was calculated from the binned data.

Single-Unit Recordings of Floccular Purkinje Cells In Vivo

Adult LTD-deficient L7-PKCi mice (n = 9) and wild-type littermates (n = 13) were prepared for chronic recording experiments and subjected to optokinetic stimulation as described in detail by De Zeeuw et al. (1998) and by Goossens et al. (2004). All preparations were done according to the European Community Council Directive (86/609/EEC) and approved by the Dutch Ethical Committee (DEC) for animal experiments. In brief, the animals were anesthetized, and they received a pedestal and a recording chamber placed over the paramedian lobule of the cerebellum. Subsequently, the animals were allowed to recover for a period of 3–4 days, and extracellular Purkinje-cell activity was recorded from the left flocculus. The electrophysiological signals were amplified, filtered, digitized, and analyzed with MATLAB (Cyberamp and CED 1401 plus units, CED; Mathworks). Single units were identified by the presence of a clean pause in simple-spike firing of at least 5 ms after the occurrence of a complex spike. The simple-spike activity was recorded during both spontaneous activity in the dark and optokinetic stimulation. Binocular visual stimulation was provided by a drum consisting of a random, black-and-white pattern rotating with an amplitude of 5° at 0.05 Hz or 0.2 Hz. Once a floccular Purkinje cell was isolated, the preferred axis of modulation was determined by rotating the optokinetic stimulus around the vertical axis or a horizontal axis at 135° azimuth, ipsilateral to the side of the recording. Only Purkinje cells with a preferred rotation around the vertical axis were used for the present study. Cumulative probabilities of simple-spike interspike intervals were calculated with all interspike intervals per stimulus condition.

Supplemental Data

The Supplemental Data for this article can be found online at http://www.neuron.org/cgi/content/full/54/1/121/DC1/.

ACKNOWLEDGMENTS

Many thanks to Reinoud Maex for helpful discussions. V.S. is grateful for a Human Frontier Science Program Long-Term Fellowship and to the Medical Research Council (0400598; R.A.S.), which provided him with financial support. The work was also supported by grants from the National Fund for Scientific Research (FWO; Belgium) and the University of Antwerp (EDS), the European Commission (QLRT-2001-2256; C.I.D.Z., E.D.S., M.H. and R.A.S.), the Dutch Organization for Medical Sciences (ZON-MW), Life Sciences (NWO-ALW), Senter (Neuro-Bsik), Prinses Beatrix Fonds (C.I.D.Z.), an EUR-fellowship of the Erasmus University Rotterdam (F.E.H.), and the Gatsby Foundation (M.H.). R.A.S. and M.H. are in receipt of Wellcome Trust Senior Research Fellowships in Basic Biomedical Science.

Received: May 20, 2006
Revised: December 2, 2006
Accepted: March 16, 2007
Published: April 4, 2007

REFERENCES

Aizenman, C.D., and Linden, D.J. (1999). Regulation of the rebound depolarization and spontaneous firing patterns of deep nuclear neurons in slices of rat cerebellum. J. Neurophysiol. *82*, 1697–1709.

Aizenman, C.D., Manis, P.B., and Linden, D.J. (1998). Polarity of long-term synaptic gain change is related to postsynaptic spike firing at a cerebellar inhibitory synapse. Neuron *21*, 827–835.

Albus, J.S. (1971). A theory of cerebellar function. Math. Biosci. *10*, 25–61.

Armstrong, D.M., and Rawson, J.A. (1979). Activity patterns of cerebellar cortical neurones and climbing fibre afferents in the awake cat. J. Physiol. *289*, 425–448.

Barbour, B. (1993). Synaptic currents evoked in Purkinje cells by stimulating individual granule cells. Neuron *11*, 759–769.

Bower, J.M., and Beeman, D. (1998). The book of GENESIS: Exploring realistic neural models with the GEneral NEural SImulation System, 2nd edition (New York, NY: TELOS).

Bower, J.M., and Woolston, D.C. (1983). Congruence of spatial organization of tactile projections to granule cell and Purkinje cell layers of cerebellar hemispheres of the albino rat: Vertical organization of cerebellar cortex. J. Neurophysiol. *49*, 745–766.

Boyden, E.S., Katoh, A., Pyle, J.L., Chatila, T.A., Tsien, R.W., and Raymond, J.L. (2006). Selective engagement of plasticity mechanisms for motor memory storage. Neuron *51*, 823–834.

Brunel, N., Hakim, V., Isope, P., Nadal, J.P., and Barbour, B. (2004). Optimal information storage and the distribution of synaptic weights: Perceptron versus Purkinje cell. Neuron *43*, 745–757.

Cingolani, L.A., Gymnopoulos, M., Boccaccio, A., Stocker, M., and Pedarzani, P. (2002). Developmental regulation of small-conductance Ca2+-activated K+ channel expression and function in rat Purkinje neurons. J. Neurosci. *22*, 4456–4467.

Cohen, D., and Yarom, Y. (2000). Cerebellar on-beam and lateral inhibition: Two functionally distinct circuits. J. Neurophysiol. *83*, 1932–1940.

Czubayko, U., Sultan, F., Thier, P., and Schwarz, C. (2000). Two types of neurons in the rat cerebellar nuclei as distinguished by membrane potentials and intracellular fillings. J. Neurophysiol. *85*, 2017–2029.

Dayan, P., and Willshaw, D.J. (1991). Optimising synaptic learning rules in linear associative memories. Biol. Cybern. *65*, 253–265.

De Zeeuw, C.I., Hansel, C., Bian, F., Koekkoek, S.K., van Alphen, A.M., Linden, D.J., and Oberdick, J. (1998). Expression of a protein kinase C inhibitor in Purkinje cells blocks cerebellar LTD and adaptation of the vestibulo-ocular reflex. Neuron *20*, 495–508.

De Schutter, E., and Bower, J.M. (1994a). An active membrane model of the cerebellar Purkinje cell. I. Simulation of current clamps in slice. J. Neurophysiol. *71*, 375–400.

De Schutter, E., and Bower, J.M. (1994b). An active membrane model of the cerebellar Purkinje cell: II. Simulation of synaptic responses. J. Neurophysiol. *71*, 401–419.

De Schutter, E., and Bower, J.M. (1994c). Simulated responses of cerebellar Purkinje cells are independent of the dendritic location of granule cell synaptic inputs. Proc. Natl. Acad. Sci. USA *91*, 4736–4740.

Eccles, J.C., Ito, M., and Szentagothai, J. (1967). The cerebellum as a neuronal machine (Berlin: Springer-Verlag).

Eilers, J., Augustine, G.J., and Konnerth, A. (1995). Subthreshold synaptic Ca^{2+} signaling in fine dendrites and spines of cerebellar Purkinje neurons. Nature *373*, 155–158.

Etzion, Y., and Grossman, Y. (1998). Potassium currents modulation of calcium spike firing in dendrites of cerebellar Purkinje cells. Exp. Brain Res. *122*, 283–294.

Fox, E.A., and Gruol, D.L. (1993). Corticotropin-releasing factor suppresses the afterhyperpolarization in cerebellar Purkinje neurons. Neurosci. Lett. *149*, 103–107.

Gardette, R., Debono, M., Dupont, J.-L., and Crépel, F. (1985). Electrophysiological studies on the postnatal development of intracerebellar nuclei neurons in rat cerebellar slices maintained in vitro. I. Postsynaptic potentials. Brain Res. *19*, 47–55.

Gilbert, P.F.C. (1974). A theory that explains the function and structure of the cerebellum. Brain Res. *1974*, 1–18.

Goossens, H.H., Hoebeek, F.E., Van Alphen, A.M., Van Der Steen, J., Stahl, J.S., De Zeeuw, C.I., and Frens, M.A. (2004). Simple spike and complex spike activity of floccular Purkinje cells during the optokinetic reflex in mice lacking cerebellar long-term depression. Eur. J. Neurosci. *19*, 687–697.

Goossens, J., Daniel, H., Rancillac, A., Van der Steen, J., Oberdick, J., Crepel, F., De Zeeuw, C.I., and Frens, M.A. (2001). Expression of protein kinase C inhibitor blocks cerebellar long-term depression without

affecting Purkinje cell excitability in alert mice. J. Neurosci. *21*, 5813–5823.

Graham, B. (2001). Pattern recognition in a compartmental model of a CA1 pyramidal neuron. Network *12*, 473–492.

Hamann, M., Desarmenien, M., Desaulles, E., Bader, M.F., and Feltz, P. (1988). Quantitative evaluation of the properties of a pyridazinyl GABA derivative (SR 95531) as a GABAA competitive antagonist. An electrophysiological approach. Brain Res. *442*, 287–296.

Hansel, C., Linden, D.J., and D'Angelo, E. (2001). Beyond parallel fiber LTD: The diversity of synaptic and non-synaptic plasticity in the cerebellum. Nat. Neurosci. *4*, 467–475.

Harvey, R.J., and Napper, R.M.A. (1991). Quantitative studies of the mammalian cerebellum. Prog. Neurobiol. *36*, 437–463.

Häusser, M., and Clark, B.A. (1997). Tonic synaptic inhibition modulates neuronal output pattern and spatiotemporal synaptic integration. Neuron *19*, 665–678.

Isope, P., and Barbour, B. (2002). Properties of unitary granule cell-Purkinje cell synapses in adult rat cerebellar slices. J. Neurosci. *22*, 9668–9678.

Ito, M. (1984). The cerebellum and neural control (New York: Raven Press).

Ito, M. (1989). Long-term depression. Annu. Rev. Neurosci. *12*, 85–102.

Ito, M. (2001). Cerebellar long-term depression: Characterization, signal transduction, and functional roles. Physiol. Rev. *81*, 1143–1195.

Ito, M., Sakurai, M., and Tongroach, P. (1982). Climbing fiber induced depression of both mossy fibre responsiveness and glutamate sensitivity of cerebellar Purkinje cells. J. Physiol. *324*, 133–134.

Jaeger, D., De Schutter, E., and Bower, J.M. (1997). The role of synaptic and voltage-gated currents in the control of Purkinje cell spiking: A modeling study. J. Neurosci. *17*, 91–106.

Jahnsen, H. (1986). Electrophysiological characteristics of neurones in the guinea-pig deep cerebellar nuclei in vitro. J. Physiol. *372*, 129–147.

Jorntell, H., and Ekerot, C.F. (2002). Reciprocal bidirectional plasticity of parallel fiber receptive fields in cerebellar Purkinje cells and their afferent interneurons. Neuron *34*, 797–806.

Jorntell, H., and Ekerot, C.F. (2003). Receptive field plasticity profoundly alters the cutaneous parallel fiber synaptic input to cerebellar interneurons in vivo. J. Neurosci. *23*, 9620–9631.

Jorntell, H., and Hansel, C. (2006). Synaptic memories upside down: Bidirectional plasticity at cerebellar parallel fiber-Purkinje cell synapses. Neuron *52*, 227–238.

Kahlon, M., and Lisberger, S.G. (2000). Changes in the responses of Purkinje cells in the Floccular complex of monkeys after motor learning in smooth pursuit eye movements. J. Neurophysiol. *84*, 2954–2960.

Koekkoek, S.K., Hulscher, H.C., Dortland, B.R., Hensbroek, R.A., Elgersma, Y., Ruigrok, T.J., and De Zeeuw, C.I. (2003). Cerebellar LTD and learning-dependent timing of conditioned eyelid responses. Science *301*, 1736–1739.

Koekkoek, S.K., Yamaguchi, K., Milojkovic, B.A., Dortland, B.R., Ruigrok, T.J., Maex, R., De Graaf, W., Smit, A.E., VanderWerf, F., Bakker, C.E., et al. (2005). Deletion of FMR1 in Purkinje cells enhances parallel fiber LTD, enlarges spines, and attenuates cerebellar eyelid conditioning in Fragile X syndrome. Neuron *47*, 339–352.

Kreitzer, A.C., and Regehr, W.C. (2000). Modulation of transmission during trains at a cerebellar synapse. J. Neurosci. *20*, 1348–1357.

Lev-Ram, V., Mehta, S.B., Kleinfeld, D., and Tsien, R.Y. (2003). Reversing cerebellar long-term depression. Proc. Natl. Acad. Sci. USA *100*, 15989–15993.

Llinas, R., and Muhlethaler, M. (1988). Electrophysiology of guinea-pig cerebellar nuclear cells in the in vitro brain stem-cerebellar preparation. J. Physiol. *404*, 241–258.

Loewenstein, Y., Mahon, S., Chadderton, P., Kitamura, K., Sompolinsky, H., Yarom, Y., and Hausser, M. (2005). Bistability of cerebellar Purkinje cells modulated by sensory stimulation. Nat. Neurosci. *8*, 202–211.

Marcaggi, P., and Attwell, D. (2005). Endocannabinoid signaling depends on the spatial pattern of synapse activation. Nat. Neurosci. *8*, 776–781.

Marr, D.A. (1969). A theory of cerebellar cortex. J. Physiol. *202*, 437–470.

Mauk, M.D., Garcia, K.S., Medina, J.F., and Steele, P.M. (1998). Does cerebellar LTD mediate motor learning? Toward a resolution without a smoking gun. Neuron *20*, 359–362.

Medina, J.F., Garcia, K.S., Nores, W.L., Taylor, N.M., and Mauk, M.D. (2000). Timing mechanisms in the cerebellum: Testing predictions of a large-scale computer simulation. J. Neurosci. *20*, 5516–5525.

Mittmann, W., Koch, U., and Hausser, M. (2005). Feed-forward inhibition shapes the spike output of cerebellar Purkinje cells. J. Physiol. *563*, 369–378.

Monsivais, P., Clark, B.A., Roth, A., and Hausser, M. (2005). Determinants of action potential propagation in cerebellar Purkinje cell axons. J. Neurosci. *25*, 464–472.

Mouginot, D., and Gahwiler, B.H. (1995). Characterization of synaptic connections between cortex and deep nuclei of the rat cerebellum in vitro. Neuroscience *64*, 699–712.

Muri, R., and Knopfel, T. (1994). Activity induced elevations of intracellular calcium concentration in neurons of the deep cerebellar nuclei. J. Neurophysiol. *71*, 420–428.

Murphy, J.T., and Sabah, N.H. (1970). Spontaneous firing of cerebellar Purkinje cells in decerebrate and barbiturate anesthesized cats. Brain Res. *17*, 515–519.

Nusser, Z., Naylor, D., and Mody, I. (2001). Synapse-specific contribution of the variation of transmitter concentration to the decay of inhibitory postsynaptic currents. Biophys. J. *80*, 1251–1261.

Ohyama, T., Nores, W.L., Murphy, M., and Mauk, M.D. (2003). What the cerebellum computes. Trends Neurosci. *26*, 222–227.

Poirazi, P., and Mel, B.W. (2001). Impact of active dendrites and structural plasticity on the memory capacity of neural tissue. Neuron *29*, 779–796.

Rancillac, A., and Crepel, F. (2004). Synapses between parallel fibres and stellate cells express long-term changes in synaptic efficacy in rat cerebellum. J. Physiol. *554*, 707–720.

Sakurai, M. (1987). Synaptic modification of parallel fibre-Purkinje cell transmission in *in vitro* guinea-pig cerebellar slices. J. Physiol. *394*, 463–480.

Schonewille, M., Khosrovani, S., Winkelman, B.H., Hoebeek, F.E., De Jeu, M.T., Larsen, I.M., Van der Burg, J., Schmolesky, M.T., Frens, M.A., and De Zeeuw, C.I. (2006). Purkinje cells in awake behaving animals operate at the upstate membrane potential. Nat. Neurosci. *9*, 459–461.

Schweighofer, N., and Ferriol, G. (2000). Diffusion of nitric oxide can facilitate cerebellar learning: A simulation study. Proc. Natl. Acad. Sci. USA *97*, 10661–10665.

Shin, S.-L., and De Schutter, E. (2006). Dynamic synchronization of Purkinje cell simple spikes. J. Neurophysiol. *96*, 3485–3491.

Shin, S.-L., Rotter, S., Aertsen, A., and De Schutter, E. (2007). Stochastic description of complex and simple spike firing in cerebellar Purkinje cells. Eur. J. Neurosci. *25*, 785–794.

Silver, R.A., Momiyama, A., and Cull-Candy, S.G. (1998). Locus of frequency-dependent depression identified with multiple-probability fluctuation analysis at rat climbing fibre-Purkinje cell synapses. J. Physiol. *510*, 881–902.

Sims, R.E., and Hartell, N.A. (2005). Differences in transmission properties and susceptibility to long-term depression reveal functional specialization of ascending axon and parallel fiber synapses to Purkinje cells. J. Neurosci. *25*, 3246–3257.

Smith, S.L., and Otis, T.S. (2005). Pattern-dependent, simultaneous plasticity differentially transforms the input-output relationship of a feedforward circuit. Proc. Natl. Acad. Sci. USA *102*, 14901–14906.

Solinas, S., Maex, R., and De Schutter, E. (2006). Dendritic amplification of inhibitory postsynaptic potentials in a model Purkinje cell. Eur. J. Neurosci. *23*, 1207–1218.

Steuber, V., and De Schutter, E. (2001). Long-term depression and recognition of parallel fibre patterns in a multi-compartmental model of a cerebellar Purkinje cell. Neurocomputing *38*, 383–388.

Stuart, G.J., Dodt, H.U., and Sakmann, B. (1993). Patch-clamp recordings from the soma and dendrites of neurons in brain slices using infrared video microscopy. Pflugers Arch. *423*, 511–518.

Sultan, F., and Bower, J.M. (1998). Quantitative Golgi study of the rat cerebellar molecular layer interneurons using principal component analysis. J. Comp. Neurol. *393*, 353–373.

Thompson, R.F., and Krupa, D.J. (1994). Organization of memory traces in the mammalian brain. Annu. Rev. Neurosci. *17*, 519–549.

Wall, M.J., and Usowicz, M.M. (1998). Development of the quantal properties of evoked and spontaneous synaptic currents at a brain synapse. Nat. Neurosci. *1*, 675–682.

Walter, J.T., Alvina, K., Womack, M.D., Chevez, C., and Khodakhah, K. (2006). Decreases in the precision of Purkinje cell pacemaking cause cerebellar dysfunction and ataxia. Nat. Neurosci. *9*, 389–397.

Walter, J.T., and Khodakhah, K. (2006). The linear computational algorithm of cerebellar Purkinje cells. J. Neurosci. *26*, 12861–12872.

Wang, S.S.-H., Denk, W., and Häusser, M. (2000). Coincidence detection in single spines mediated by calcium release. Nat. Neurosci. *3*, 1266–1273.

Williams, S.R., Christensen, S.R., Stuart, G.J., and Häusser, M. (2002). Membrane potential bistability is controlled by the hyperpolarization-activated current I(H) in rat cerebellar Purkinje neurons in vitro. J. Physiol. *539*, 469–483.

Willshaw, D.J., Buneman, O.P., and Longuet-Higgins, H.C. (1969). Non-holographic associative memory. Nature *222*, 960–962.

Womack, M.D., and Khodakhah, K. (2003). Somatic and dendritic small-conductance calcium-activated potassium channels regulate the output of cerebellar purkinje neurons. J. Neurosci. *23*, 2600–2607.

Xia, J., Chung, H.J., Wihler, C., Huganir, R.L., and Linden, D.J. (2000). Cerebellar long-term depression requires PKC-regulated interactions between GluR2/3 and PDZ domain-containing proteins. Neuron *28*, 499–510.